Available online at www.sciencedirect.com

ScienceDirect

Procedia CIRP 111 (2022) 711–714

www.elsevier.com/locate/procedia

12th CIRP Conference on Photonic Technologies [LANE 2022], 4-8 September 2022, Fürth, Germany

Self-cleaning stainless steel surfaces induced by laser processing and chemical engineering

Pierre Lorenz[a,*], Joachim Zajadacz[a], Franka Marquardt[a], Martin Ehrhardt[a], Gregor Hommes[b], Sebastian Peter[b], Klaus Zimmer[a]

[a]*Leibniz Institute of Surface Engineering (IOM), Department of ultra-precision surfaces, Permoserstr. 15, Leipzig, 04318, Germany*
[b]*SKAN Deutschland GmbH, Nickrischer Str. 2, D-02827 Görlitz/Hagenwerder, Germany*

* Corresponding author. Tel.: +49-341-235-3287; fax: +49-341-235-0000. *E-mail address:* pierre.lorenz@iom-leipzig.de

Abstract

Nanostructured surfaces show a variety of beneficial macroscopic effects. The combination of hierarchic nanostructures with a suitable chemical surface composition allows for the fabrication of surfaces with interesting fluidic properties beyond such effects. This approach enables the specification of nano/microstructure and chemical composition independent of each other. Various hierarchical micro- and nanostructures can be realized by laser texturing of stainless steel surfaces with infrared picosecond laser. Simultaneously, the surface is activated for chemical processing. The surface can now be tuned by bonding of a self-assembled monolayer on the laser-treated surface by chemical treatment. This two-step functionalization process allows the for separated adjusting of the surface topography and chemical composition and thus for the well-defined setting of the surface properties. The fabrication of superhydrophobic surfaces with self-cleaning properties are performed that can be functionalized further by subsequent laser-irradiation. Furthermore, the long-time stability of the surface functionalization in relation to the impact chemicals or radiation was investigated.

Keywords: nanostructuring; stainless steel; superhydrophobic; self-assembled monolayer; SAM

1. Introduction

Water repellent, self-cleaning and ant-icing surface properties are related to the wetting properties of surfaces that result from the chemical composition of the near surface and the surface topography/morphology e.g.laser treatment allows the fabrication of suitable surfaces [1, 2]. The most important models describing the wetting of surfaces are the Young, Wenzel and the Cassie-Baxter models (see [3]). It is considered as a general rule that the surface morphology enhances the fundamental wetting behavior of the material given by the material properties. The surface energy can be considered as a relevant measure for the fundamental material wetting behavior. Laser irradiation and laser ablation are known to cause near-surface material modifications in addition to their texturing/patterning capabilities. These effects can be achieved in almost any material [4]. Ablation, texturing and modification of steel and in particular stainless steel by laser irradiation has been studied extensively [5-10]. Depending on the laser processing parameters and processing strategies various micro/nanostructures surfaces can be realized. This variety of patterns including spot size micron patterns, melting features and nano patterns from redeposition or self-organization processes can form hierarchical structures across scales. It is widely accepted that hierarchical textured surfaces similar to the natural prototype (e.g. Lotus leaf) show convincing superhydrophobic properties [5, 11]. The modification of metal surfaces in relation to their wetting behavior after laser irradiation was studied by Kitzig et al. [12]. The gradual rise of the hydrophobicity with time and a saturation after months was

10.1016/j.procir.2022.08.019

observed for different metals. The change of the wettability of surfaces with time is also well known which is often related to the deposition of air-born molecules or the wetting by water [5]. A specific catalytic activity of laser textured surfaces is suggested to be responsible for a surface enrichment with carbon that provides the hydrophobic properties of the surface resulting in superhydrophobic properties together with the surface structure [6, 12]. Heat accumulation during ps-laser ablation can contribute to the surface modification of SST [13]. However, the standard approach for the creation of superhydrophobic surfaces is the chemical functionalization after patterning. Silicon or other dielectric oxides can be treated by functional silanes whereas a fluorinated long-backbone alkane often provides the low surface energy needed for superhydrophobicity. The key issue for a stabile functionalization with self-assembled monolayers is the covalent bond formation with the host material after texturing [14]. For different metal oxides a chemical modification by phosphonic acid modified alkanes is preferred [15, 16]. In addition to the general fields of application for self-cleaning or anti-icing, specific applications call for localized functionalizations for liquid pinning, localized deposition or liquid transport applications. Lasers may be helpful for patterning to realize localized hydrophilic/hydrophobic areas. In this study, the hybrid functionalization (laser structuring and chemical modification) and its time-dependent chemical stability in 50 % H_2O_2 especially dependent on the laser parameter was studied. Furthermore, the self-cleaning of the hybrid functionalized stainless steel was studied.

2. Experimental Set-up

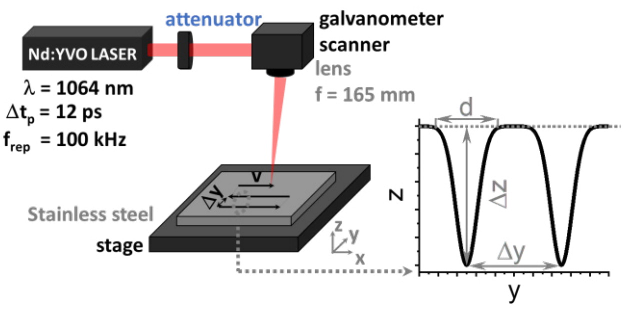

(a)

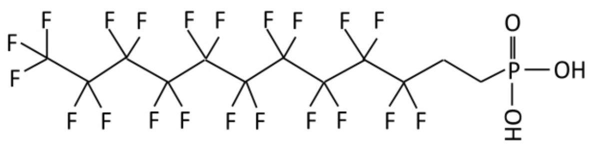

(b)

Fig. 1. (a) Schematic illustration of the laser treatment process
(b) Illustration of the (1H,1H,2H,2H-perfluorododecyl) phosphonic acid (F21) molecule $C_{10}H_6F_{17}O_3P$

The functionalization of stainless steel (SST) (type: 316 , ground and cleaned) was performed in a two-step process. In step 1, the stainless steel surface was irradiated by an infrared ps laser with a wavelength of λ = 1064 nm, a pulse duration of Δt_p =12 ps and a repetition rate of f_{rep} = 100 kHz. For areal laser processing, the laser beam was focused by a f-theta lens with a focal length f = 165 mm and was moved in parallel lines with a line distance Δy over the sample surface by a scanner. The schema of the scanning procedure is given in Fig. 1 (a). SST surfaces were irradiated with different scanning speeds v (100 to 700 mm/s) and different laser power P (0.9 to 2.2 W) but with a fixed line distance of Δy = 10 µm. The accumulated laser fluence can be estimated by:

$$\Phi_{acc} = \frac{P}{v \cdot \Delta y} \quad (1)$$

After the laser irradiation the stainless steel surface was cleaned by ultrasonification in an isopropanol water solution (1:1) for 15 min. In the second step, the laser-structured and cleaned stainless steel surface was chemically modified. Therefore, the samples were placed in a (1H,1H,2H,2H-perfluorododecyl) phosphonic acid (F21) /tetrahydro- furan (THF) solution with a F21-concentration of 0.8 mmol/l for 2 h at room temperature. Finally, the samples were flushed with isopropanol, dried in a nitrogen stream and annealed at 85 °C for 10 min. The covalent bonding of a F21 molecule forming a self-assembling monolayer (SAM) to the laser-treated stainless steel surface causes a stable chemical functionalization of the surface. In Fig.1(b) the chemical structure of the F21 molecule is shown. The morphology of the functionalized surface was analyzed by optical and scanning electron microscopy (SEM). The wetting behavior was evaluated by water contact angle measurements. Furthermore, the longtime stability of the F21 SAM layer in a 50 % H_2O_2 solution was studied by repeating water contact angle measurements after exposure to H_2O_2. The water-droplet induced self-cleaning of the functionalized stainless steel surface from organic particles was studied. For this purpose, garlic granules with sub-mm particles were applied to the surface of the functionalized stainless steel samples. The stainless steel samples was tilted at angle of ~14° and a water droplet with a volume of 7 µl was applied to the sample surface. The resulting modification of the particle distribution was optical determined.

3. Results

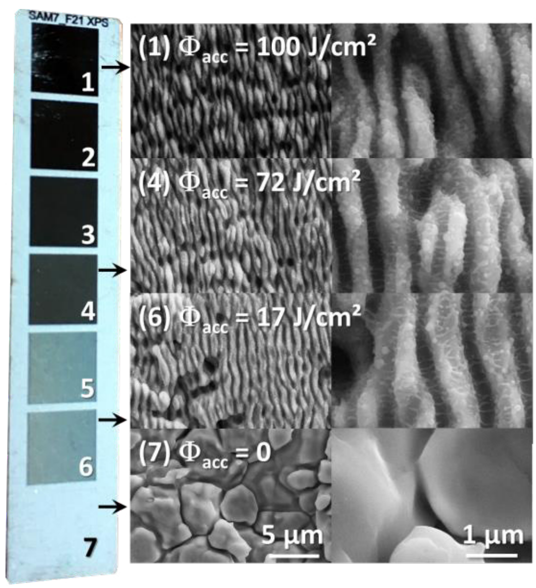

Fig. 2. (left) Optical image of laser treated surface and (right) exemplary SEM images of laser treated surfaces at different Φ_{acc}.

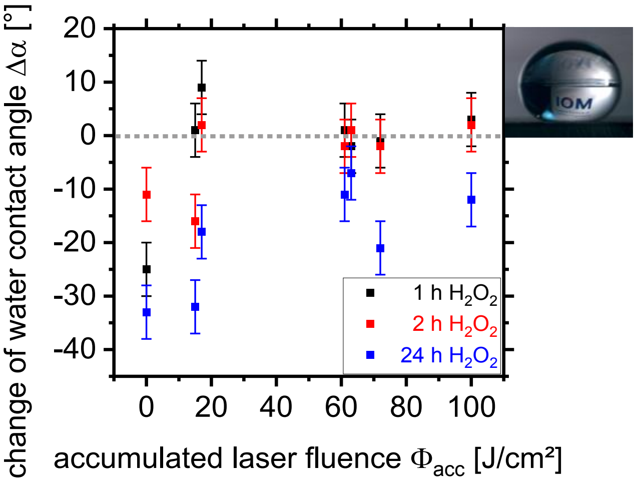

Fig. 3. Change of the water contact angle (WCA) depending on the accumulated laser fluence at different times and an exemplary image of a water droplet on a functionalized pristine surface

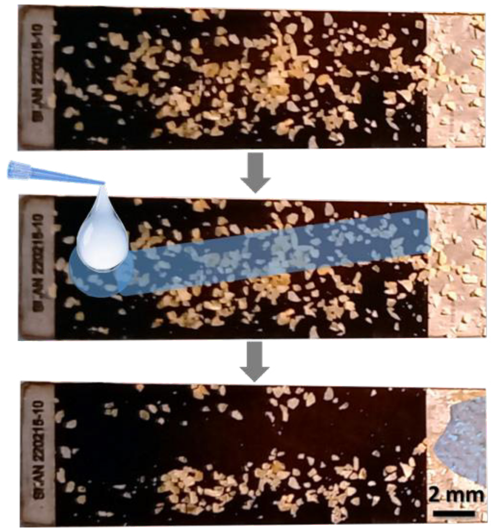

Fig. 4. (top) optical image of organic particles on functionalized stainless steel surface (dark area)
(middle) Schematic illustration of the path of the water droplet (blue marked area)
(bottom) optical image of functionalized stainless steel surfaces after droplet transition (blue marked sticked water droplet)

The arrangement of different fields on stainless steel to study the impact of processing parameters is shown in Fig. 2 (left). There, a distinct change in the optical appearance after laser treatment is seen; obviously an increasing light trapping is achieved with increasing accumulated laser fluence. This can be related to the laser-induced surface topography/morphology or chemical modifications of the stainless steel surface. Exemplary SEM images of the surface morphology are summarized in Fig. 2 that show different micro- and nanostructured surface features. Typical surface morphologies are micro needles, LIPSS and melting structures. In particular, the formation of laser-induced periodic surface structures (LIPSS) with a period of ~ 920 nm (see Fig. 2 (6)) are observed to enable a hierarchical structure. After laser texturing the water contact angle drops below 10° for all relevant laser texturing conditions. Untreated stainless steel samples show a water contact angle of (65 ± 5)° that rises after functionalization with F21 to (136 ± 5)°. As expected, feature the laser textured, functionalized surface a superhydrophobic behavior with an average water contact angle of ~ 150° (area 1-5). The differences of the measured water contact angle – 130° to 155° – are related to different laser processing conditions according to Fig. 3. The stability of such superhydrophobic surfaces is of high practical importance, therefore the degradation of the superhydrophobic properties by immersion in different solutions (NH_4OH, H_2O_2, NaCl) was studied. the functionalized stainless steel samples were placed in a chemical solution for a defined time and the water contact angle was measured after defined time steps. Here we report on the stability of the superhydrophobic SST to H_2O_2 as a strong oxidizing agent for materials. After immersion for 1 day the samples were cleaned and dried before the water contact angle was determined. The change of the water contact angle in dependence on the accumulated laser fluence for different H_2O_2 exposure times is summarized in Fig. 3. As shown, the contact angle is depending on the accumulated laser fluence that also determines the surface structure. In general, with stronger exposures the surface is increasingly textured (micro/nanostructures) and the water contact angle increases.

In addition, the sensitivity with respect to the H_2O_2 solution decreases as changes of the contact angle are less pronounced for samples processed with a high accumulated laser fluence. Further, the change of the water contact angle increased at increasing H_2O_2 exposure time. The non-irradiated surface presented a distinct reduction of the water contact angle after 1 h H_2O_2 exposure time where the laser-treated surface at Φ_{acc} = 100 J/cm² presented a slight reduction of the water contact angle after 24 h. One possible practical application of superhydrophobic stainless steel surfaces is the self-cleaning effect known from nature. The self-cleaning effect of the stainless steel surface from organic particles was tested. An exemplary result of a self-cleaning process is summarized in Fig. 4. In Fig. 4 (top) the functionalized stainless steel surface covered in sub-mm organic particles is shown. A water droplet was applied on the left side of the sample and due to gravity force (the sample was tilted at 14°) the water droplet was sliding to the right side of the sample. The path of the water droplet is schematically illustrated in Fig. 4 (middle). The roll off of the water droplet resulted in a removal of the organic particles in its path (see Fig. 4 (bottom)). The water particles pick up organic particles due to their hydrophilic nature and remove them from the surface. After leaving the textured area the water droplet stuck to the functionalized but not laser textured surface (see Fig. 4 (bottom) blue marked area). At non-treated metal surfaces with a water contact angle of 65° the water droplet sticks at the surface already at high tilt angles. That means, a water-droplet induced self-cleaning process cannot be induced.

4. Discussion

The laser modification of the SST during the texturing process includes a number of processes: laser ablation for microstructure (topography), nanostructure formation (e.g. by LIPSS), chemical surface modification by oxidation or redeposition processes and structural alterations due to ablation and heating effects. The strength of these effects changes with laser processing conditions and processing strategy. Hence, the properties of the SST surface for the functionalization procedure may be changed in addition to the surface morphology/topography. Hence, both topographical as well as chemical properties are influenced by the accumulated laser fluence in a complex manner. In relation to the measured water contact angles a transition from Wenzel state to the Cassie-Baxter state with increasing accumulated laser fluence is suggested. Obviously, the degradation speed of the superhydrophobic properties due to liquid H_2O_2 exposure depends also on the accumulated laser fluence. The observed WCA alterations upon H_2O_2 exposure need to discuss nanoscopic alteration as SEM studies show no differences in the surface morphology after degradation. H_2O_2 exposure can cause the oxidation of organic as well as inorganic materials at the contact area of the liquid H_2O_2 with the surface. The most relevant effect expected for the F21 molecule is the degradation of the backbone that results in the reduction of the fluorine content. In relation to the WCA or the wetting state a different contact area of the H_2O_2 with the F21-modified SST surface is likely. The higher the contact area the faster the degradation happens. With that the dependency of the WCA as well as the reduction of the WCA upon H_2O_2 exposure can be understood. Considering for simplicity the alteration of the SST morphology with the accumulated laser fluence the dependence on the laser texture parameters can be realized. Topographic effects explain the different contact angle of the untreated surface and the laser treated surface especially at higher. Considering the high water contact angles a Cassie-Baxter state where the tops of the needles are in contact with the liquid can be expected. Due to the Laplace pressure the upper part of the needles are in contact with a liquid in Cassie-Baxter state. For the H_2O_2 solutions only the wetted parts of pillars suffer degradation whereas not-wetted parts stay unchanged. This approach can explain the gradual reduction of the water contact angle for prolonged H_2O_2 exposure experiments. The experiments performed have shown that the degradation sensitivity of the functionalization (reduction of the water contact angle) of the stainless steel sample with respect to H_2O_2 exposure decreases with increasing accumulated laser fluence. The laser power used are above the ablation threshold and generate an ablation process on the stainless steel surface where the redeposition leads to the formation of nanostructures on the surface. It can be assumed that the increase of the accumulated laser fluence leads to an increase of the ablated mass and thus to an increase of the redeposited material. This dependence could be found for e.g. copper [17]. The redeposited stainless steel material most likely leads to the formation of a non-compact sponge-like layer as in the case of other metals [17]. The results show the trend that the increasing of a nanostructured layer result in a reduction of the sensitivity of the functionalization. TEM measurements are necessary to clarify this model idea. One possible approach to explain the accumulated laser fluence dependence is the partial coverage of the functionalized stainless steel sample with the H_2O_2 solution due to air trapping [18] on the functionalized stainless steel surface. The gas phase formation most likely reduced the degradation effect.

5. Conclusion

Optimized laser texturing with an appropriate chemical functionalization can provide conditions to realize superhydrophobic surfaces with WCA exceeding 150°. In particular, chemical functionalized, hierarchical surface morphology provides not only superhydrophobic but also self-cleaning effects. The achieved functionalized SST feature a good resistance to 50% H_2O_2 solutions. The strong attack of H_2O_2 reduced the WCA gradually which can be explained by the degradation of the functionalization at the topographical tips of the hierarchical structures which finally cause a transition from the Cassie-Baxter to the Wenzel state and the collapse of the superhydrophobic properties. Based on the current results stable wetting properties for various applications can be realized.

Acknowledgements

This work is supported in parts by Europäische Fonds für regionale Entwicklung (EFRE) and the Freistaat Sachsen in frame of the contract Nr. 100387051.

References

[1] Chen F, et al. Bioinspired Wetting Surface via Laser Microfabrication. ACS Applied Materials & Interfaces, 2013; 5:6777-6792.
[2] Yao C, et al. A Simple Way to Achieve Self-Cleaning Surfaces with Unique Antifouling Property. Journal of Chemistry, 2020; 2020:9072432.
[3] Barati Darband G, et al. Science and Engineering of Superhydrophobic Surfaces: Review of Corrosion Resistance, Chemical and Mechanical Stability. Arabian Journal of Chemistry, 2020; 13:1763-1802.
[4] Bäuerle D. Laser processing and chemistry: Springer Science & Business Media; 2013.
[5] Gregorcic P, et al. Long-Term Influence of Laser-Processing Parameters on (Super)hydrophobicity Development and Stability of Stainless-Steel Surfaces. Materials, 2018; 11:
[6] Wang X C, et al. Picosecond Laser Surface Texturing of a Stavax Steel Substrate for Wettability Control. Engineering, 2018; 4:816-821.
[7] Razi S, et al. Birth of periodic Micro/Nano structures on 316L stainless steel surface following femtosecond laser irradiation; single and multi scanning study. Optics & Laser Technology, 2018; 104:8-16.
[8] Mai T A, et al. Micromelting and its effects on surface topography and properties in laser polishing of stainless steel. Journal of Laser Applications, 2004; 16:221-228.
[9] Li Z L, et al. Analysis of oxide formation induced by UV laser coloration of stainless steel. Applied Surface Science, 2009; 256:1582-1588.
[10] Wu B, et al. Superhydrophobic surfaces fabricated by microstructuring of stainless steel using a femtosecond laser. Applied Surface Science, 2009; 256:61-66.
[11] Gregorcic P, et al. Controlling the stainless steel surface wettability by nanosecond direct laser texturing at high fluences. Appl. Phys. A, 2017; 123:
[12] Kietzig A M, et al. Patterned superhydrophobic metallic surfaces. Langmuir, 2009; 25:4821.
[13] Faas S, et al. Heat accumulation controlled surface functionalization of stainless steel with structuring rates up to 500 mm2/s. Procedia CIRP, 2018; 74:324-327.
[14] Silberzan P, et al. Silanation of silica surfaces. A new method of constructing pure or mixed monolayers. Langmuir, 1991; 7:1647-1651.
[15] Raman A, et al. Formation of Self-Assembled Monolayers of Alkylphosphonic Acid on the Native Oxide Surface of SS316L. Langmuir, 2006; 22:6469-6472.
[16] Quiñones R, et al. Study of Perfluorophosphonic Acid Surface Modifications on Zinc Oxide Nanoparticles. Materials (Basel), 2017; 10:
[17] Lorenz P, et al. Secondary electron yield reduction of copper after 355 nm ultrashort pulse laser ablation. Lasers in Manufacturing and Materials Processing, 2022;
[18] Zhang Y, et al. Superhydrophobic engineering surfaces with tunable air-trapping ability. J. Micromech. Microeng., 2008; 18:035024.